Internal Glucose Residue Loss in Protonated *O*-Diglycosyl Flavonoids upon Low-Energy Collision-Induced Dissociation

Yu-Liang Ma, Irina Vedernikova, Hilde Van den Heuvel, and Magda Claeys
Department of Pharmaceutical Sciences, University of Antwerp (UIA), Antwerp, Belgium

The low-energy collision-induced dissociation of protonated flavonoid *O*-diglycosides, i.e., flavonoid *O*-rutinosides and *O*-neohesperidosides, containing different aglycone types has been studied. The results indicate that the unusual $[M + H - 162]^+$ ion formed by internal glucose residue loss, which in a previous study was shown to be a rearrangement ion, is strongly dependent upon the aglycone type. For 7-*O*-diglycosides, the internal glucose loss is very pronounced for aglycones of the flavanone type, but is completely absent for aglycones of the flavone and flavonol types. Internal glucose residue loss was found to correspond to a minor fragmentation pathway for flavonol 3-*O*-diglycosides. A plausible mechanism is proposed based on proton mobilization from the aglycone to the disaccharidic part of the flavonoid *O*-diglycosides which is supported by theoretical calculations and model building. (J Am Soc Mass Spectrom 2000, 11, 136–144) © 2000 American Society for Mass Spectrometry

Flavonoid glycosides are predominant forms of naturally occurring flavonoids in plants, representing a large group of secondary plant metabolites. They all contain a C_{15} flavonoid as an aglycone, are usually divided into *O*- and *C*-glycosyl flavonoids, and are of interest because they have biological activities, are useful for chemotaxonomy, and are used as tracers in medicinal plant preparations [1, 2].

During recent years, efforts in our laboratory have been devoted to the structural analysis of *O*- and *C*-glycosyl flavonoids isolated from medicinal herbs using fast atom bombardment (FAB) in combination with collision-induced dissociation (CID) and tandem mass spectrometry (MS/MS) [3–6]. In the present study, we have re-investigated some *O*-diglycosyl flavonoids with the aim to characterize their mass spectrometric behaviors in more detail. The term *O*-diglycosyl flavonoid (or flavonoid *O*-diglycoside) is used to denote a glycosylated flavonoid having a disaccharide attached to a hydroxyl group of the aglycone nucleus via its anomeric (C-1) carbon. The samples selected for this study were 7-*O*-diglycosyl flavones (**1** and **2**), flavonols (**3**), flavanones (**4**–**6**), and 3-*O*-diglycosyl flavonols (**7** and **8**), making up four pairs of isomers (Figure 1). The glycan part was either a rutinose [rhamnosyl-(α1 → 6)-glucose] or a neohesperidose [rhamnosyl-(α1 → 2)-glucose], which are the two most common disaccharides found in association with flavonoids [1]. These compounds, including hesperidin (**6**) and rutin (**8**), are of particular interest because they are health-related bioflavonoids [7, 8], which have antioxidant and free radical scavenging activity [9], have been shown to reduce the risk of cancer and cardiovascular diseases [8, 10, 11], and are regularly encountered in biological and phytochemical analyses of plant extracts.

With regard to the mass spectrometric behavior of the selected *O*-diglycosyl flavonoids special emphasis has been given to the phenomenon of internal monosaccharide residue loss, which can give false glycan sequence information and has been described for protonated 1,2- and 1,6-linked tri- and tetrasaccharides [12–14], branched oligosaccharides [15], and anthracycline aminosaccharides [16].

The phenomenon of internal monosaccharide residue loss was first discussed in detail by Kováčik et al. [12] who examined a protonated tetrasaccharide α-L-Rha-(1 → 3)-α-L-Rha-(1 → 2)-α-D-Gal-(1 → 3)-α-D-GlcNAc-OMe and related oligosaccharides under high-energy CID conditions and found evidence for elimination of the internal galactose residue. A simple mechanism corresponding to a charge-remote rearrangement and elimination of the 1 → 2 substituted galactose was proposed. In a following study Brüll et al. [13] showed that internal monosaccharide residue loss is not limited to ions containing 1 → 2 substituted monosaccharide residues but also occurs in ions of trisaccharides that have 1 → 6 linked monosaccharide residues. Internal monosaccharide residue loss was reported by Ernst et al. [15] for electrospray (ES)-generated $[M + H]^+$ and $[M + NH_4]^+$ ions of sialyl-

Address reprint requests to Magda Claeys, Department of Pharmaceutical Sciences, University of Antwerp (UIA), Universiteitsplein 1, B-2610 Antwerp, Belgium. E-mail: claeys@uia.ua.ac.be

1044-0305/00/$20.00
PII S1044-0305(99)00133-6

Received June 9, 1999
Revised October 14, 1999
Accepted October 19, 1999

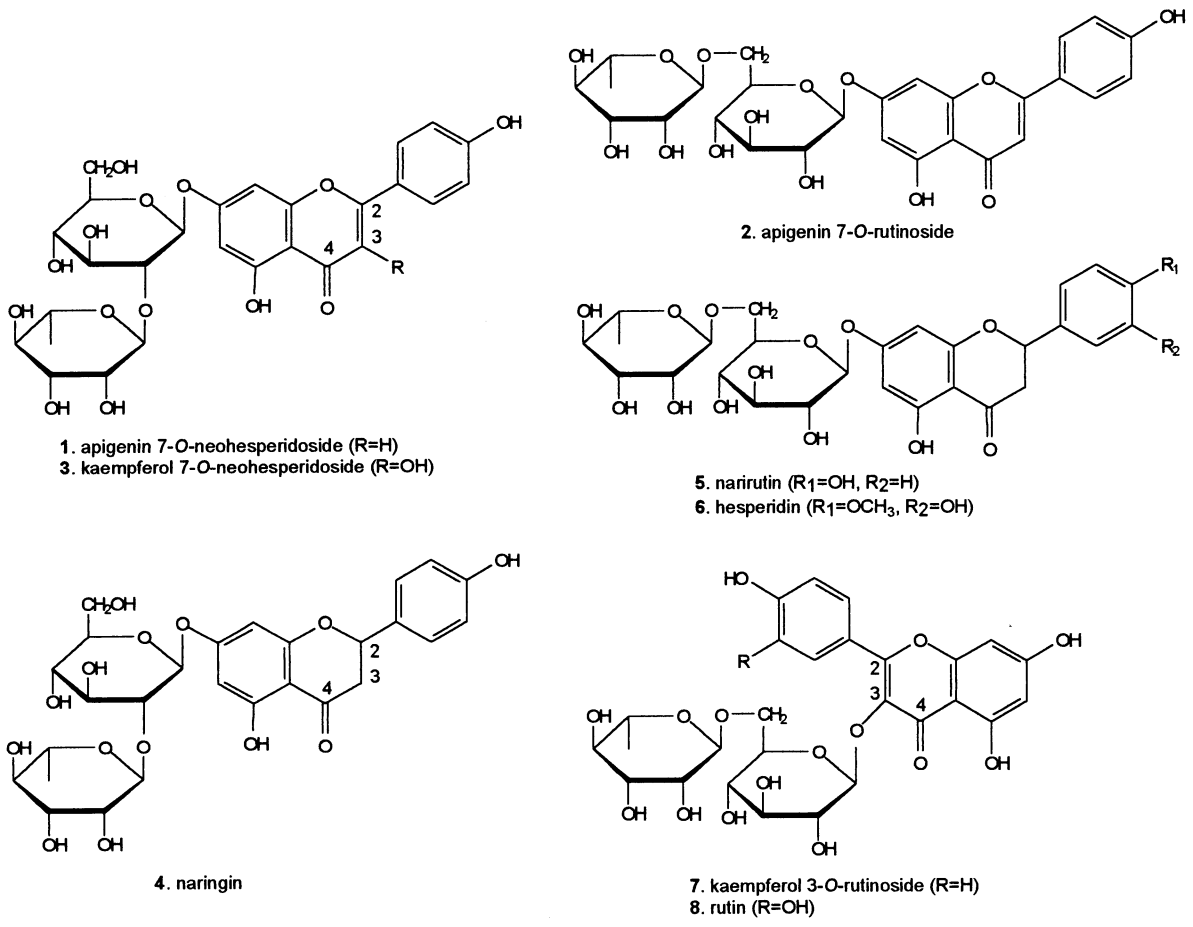

Figure 1. Structures of the *O*-diglycosyl flavonoids (**1**–**8**) investigated.

Lewis-type oligosaccharides under low-energy CID conditions. The internal monosaccharide residue loss was rationalized by poor charge fixation and enhanced internal proton mobility resulting in sequence-isomerized $[M + H]^+$ ions in which subsequently a migration of a fucosyl C1 carbonium ion towards a sialyl residue takes place. The role of the proton in internal monosaccharide residue loss was supported by a study by Brüll et al. [14] who demonstrated that sodium-cationized and deprotonated oligosaccharides do not undergo this loss. In addition, the loss of an internal monosaccharide residue has recently been studied in detail by Warrack et al. [16] for both ES- and FAB-generated protonated anthracycline aminodisaccharides containing a terminal 3-aminofucose and an internal fucose residue under low- and high-energy CID conditions. Examination of the peracetylated derivative and the deuterated analog revealed that the internal fucose residue loss is due to a rearrangement process.

Experimental

Materials

The six 7-*O*-diglycosyl flavonoids (**1**–**6**) and two 3-*O*-diglycosyl flavonols (**7** and **8**) investigated in this study are apigenin 7-*O*-neohesperidoside (**1**), apigenin 7-*O*-rutinoside (**2**), kaempferol 7-*O*-neohesperidoside (**3**), naringenin 7-*O*-neohesperidoside (**4**), naringenin 7-*O*-rutinoside (**5**), hesperitin 7-*O*-rutinoside (**6**), kaempferol 3-*O*-rutinoside (**7**), and quercetin 3-*O*-rutinoside (**8**) (structures shown in Figure 1 and trivial names given in Table 1). Compounds **1**, **3**, **4**, **6**, **7**, and **8** were purchased from Roth (Karlsruhe, Germany), whereas **2** and **5** were from Extrasynthèse (Genay, France). The purity, greater than 95% for all compounds except **6** whose purity was 83% (at 340 nm), was confirmed by reverse-phase high performance liquid chromatography (RP-HPLC). HPLC analysis was performed using an instrument consisting of a Waters 600MS solvent delivery system (Waters, Milford, MA), a Rheodyne valve with an injection volume of 100 μL (Achrom, Cotati, CA) and a Waters 991 photodiode array detector. A ChromSpher 5 C_{18} HPLC column (200 mm $\times$ 3 mm i.d.) from Chrompack (Middelburg, The Netherlands) was employed. The mobile phase was a two solvent system consisting of solvent A (1% formic acid in Milli-Q water) and solvent B (1% formic acid in HPLC grade acetonitrile). The gradient profile applied was: 0–10 min linear gradient from 90% to 80% A, 10–28 min linear gradient to 70% A, 28–31 min to 0% A, 31–37 min isocratically at 0% A,

Table 1. Compounds investigated and the *m/z* values of $[M + H]^+$ ions and major fragment ions in their positive ion FAB mass spectra

Flavonoid *O*-diglycosides[a]	No.	M_r	$[M + H]^+$	Y_0	Y_1	Y*
Apigenin 7-*O*-neohesperidoside (rhoifolin)[b]	**1**	578	579	271	—	—
Apigenin 7-*O*-rutinoside (isorhoifolin)	**2**	578	579	271	433w[c]	—
Kaempferol 7-*O*-neohesperidoside	**3**	594	595	287	—	—
Naringenin 7-*O*-neohesperidoside (naringin)	**4**	580	581	273	—	—
Naringenin 7-*O*-rutinoside (narirutin)	**5**	580	581	273	435w	419w
Hesperitin 7-*O*-rutinoside (hesperidin)	**6**	610	611	303	465w	449w
Kaempferol 3-*O*-rutinoside (nicotiflorin)	**7**	594	595	287	449w	—
Quercetin 3-*O*-rutinoside (rutin)	**8**	610	611	303	465w	—

[a]Neohesperidoside: rhamnosyl-(α1 → 2)-glucoside. Rutinoside: rhamnosyl-(α1 → 6)-glucoside.
[b]Trivial name is given in parentheses.
[c]w—weak.

37–40 min linear gradient to 90% A, 40–50 min isocratically at 90% A. The flow rate was 0.4 mL/min. On-line UV spectra were recorded between 220 and 400 nm and the chromatograms were constructed at 280 nm. Peak purity tests were performed using the Waters Millennium 2.0 software. Under the RP-HPLC conditions used the retention times were 19.16 (**1**), 18.31 (**2**), 18.79 (**3**), 19.00 (**4**), 17.75 (**5**), 16.69 (**6**), 17.79 (**7**), and 15.29 min (**8**). Critical isomeric pairs containing the same aglycone part such as **1**/**2**, **3**/**7**, and **4**/**5** showed retention time differences of 0.85, 1.00, and 1.25 min, respectively, and were fully resolved. Neohesperidosides eluted earlier than the corresponding rutinosides, a chromatographic behavior which was documented in a study by Vande Casteele et al. [17].

Mass Spectrometry

All spectra were obtained on a VG 70-SEQ (Micromass, Manchester, UK) hybrid mass spectrometer with EBqQ configuration, equipped with a cesium ion source. The acronym FAB is used to refer to cesium ion bombardment. The samples were dissolved in methanol or a methanol-dimethylsulphoxide (DMSO) mixture (1:1; v/v). A eutectic mixture of dithiothreitol and dithioerythritol [5:1; w/w], denoted as "magic bullet," was used as liquid matrix. For recording low-energy CID spectra of protonated molecules, precursor ions were mass selected with a resolution of about 1000 using the magnetic sector. CID was performed in the quadrupole gas cell with argon as collision gas at a pressure of approximately 5×10^{-6} mbar (measured in the quadrupole housing) and using a collision energy of 30 eV except if mentioned otherwise. At these conditions multiple collisions occur and the precursor ion beam was reduced to approximately 60% of its original value. The product ion spectra were obtained in the continuous mode of acquisition of the quadrupole analyzer. Sequence ion notations according to Domon and Costello [18] have been used, e.g., the Y_1 and Y_0 ions correspond to the $[M + H - 146]^+$ and $[M + H - (146 + 162)]^+$ ions, respectively. The latter ion represents the protonated aglycone.

Theoretical Calculations

Theoretical calculations were performed with the semiempirical AM1 method employing MOPAC 6.0 software [19] in Insight II (MSI/BIOSYM, San Diego, CA, 1995). The conformational analysis of flavonoid aglycones was investigated as follows: in a first step, the geometry of model compounds, i.e., 7-*O*-methyl ethers of apigenin (**9**), kaempferol (**10**), and naringenin (**11**), was optimized, and in a second step, the geometry optimization was done for the protonated molecule. Minimum energy conformers were used in both steps and quantum chemical properties for ground and protonated states are represented by molecular electrostatic potential (MEP) maps and proton affinities (PA), respectively.

Results and Discussion

Previous work in our laboratory revealed that "magic bullet" is a suitable liquid matrix for recording FAB spectra of *O*- and *C*-glycosyl flavonoids. An advantage is that the spectra obtained with this matrix show less chemical noise interfering with analyte signals in the molecular mass range compared to other matrices. Abundant protonated molecules, $[M + H]^+$ ions, and protonated aglycones, Y_0 ions (base peaks), at *m/z* 579 and 271 for **1** and **2**, *m/z* 595 and 287 for **3** and **7**, *m/z* 581 and 273 for **4** and **5**, *m/z* 611 and 303 for **6** and **8** were observed in the positive ion FAB mass spectra (Table 1). These results are in agreement with their molecular weights and their aglycone constituents, and are also consistent with available literature data [5, 20–23]. The Y_1 ion was very weak for the three *O*-neohesperidosides (**1**, **3**, and **4**) but relatively abundant for the five *O*-rutinosides (**2** and **5**–**8**). For **5** and **6**, this ion was accompanied by an ion (labeled as **Y***) 16 mass units lower. Because the **Y*** ion, i.e., $[M + H - 162]^+$, corresponds to the loss of a hexose (glucose) residue from precursor $[M + H]^+$ ions, the conclusion can be drawn that first-order positive ion FAB spectra may give ambiguous information on the carbohydrate sequence for *O*-diglycosyl flavonoids.

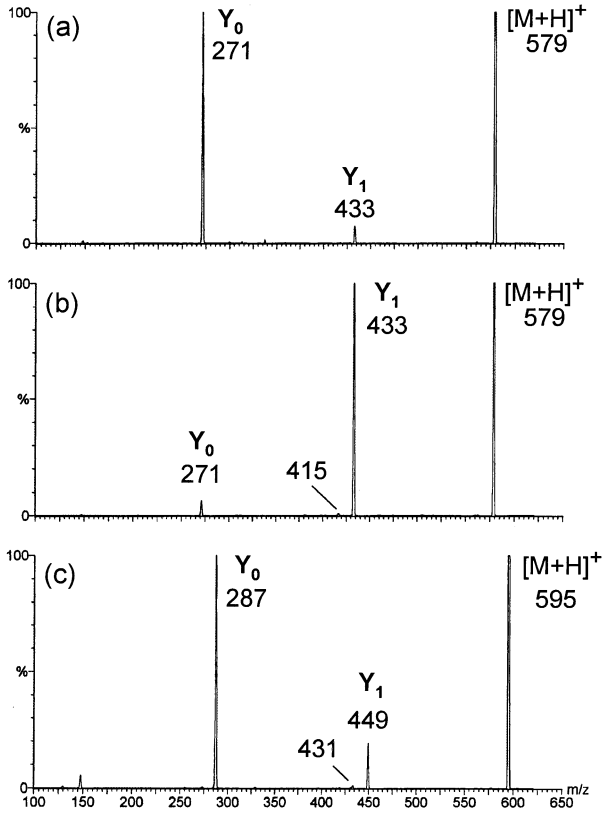

Figure 2. CID product ion spectra obtained for $[M + H]^+$ ions of (**a**) apigenin 7-*O*-neohesperidoside (**1**), (**b**) apigenin 7-*O*-rutinoside (**2**), and (**c**) kaempferol 7-*O*-neohesperidoside (**3**), respectively. The spectra are normalized to the most abundant product ion. The relative abundances of these ions are (**a**) 33%, (**b**) 76%, and (**c**) 33%, respectively.

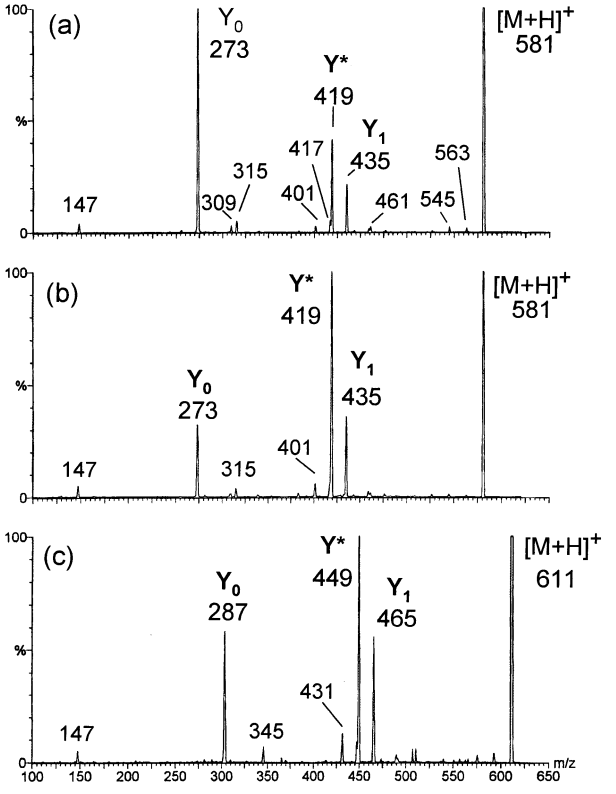

Figure 3. CID product ion spectra obtained for $[M + H]^+$ ions of (**a**) naringenin 7-*O*-neohesperidoside (**4**), (**b**) naringenin 7-*O*-rutinoside (**5**), and (**c**) hesperitin 7-*O*-rutinoside (**6**), respectively. The spectra are normalized to the most abundant product ion. The relative abundances of these ions are (**a**) 26%, (**b**) 56%, and (**c**) 14%, respectively.

Low-Energy CID of $[M + H]^+$ Ions

The low-energy CID product ion spectra of protonated 7-*O*-diglycosides of the flavone (**1** and **2**) and flavonol (**3**) types are presented in Figure 2a–c. The fragmentations observed for protonated **1**–**3** are very simple, i.e., cleavage at two glycosidic bonds results in two major ions $\mathbf{Y_0}$ and $\mathbf{Y_1}$ at *m/z* 271 and 433 for **1** and **2** (Figure 2a, b) and at *m/z* 287 and 449 for **3** (Figure 2c), respectively. The complementary **B** type ions are absent or have a low relative abundance. In these three cases, the glycan sequence, i.e., deoxyhexose-hexose-flavonoid, can be unambiguously determined. In addition, the CID spectra also indicate that the very simple spectral pattern is neither affected by a hydroxyl substitution at C-3 of the aglycone (e.g., **1** and **3**), nor by the interglycosidic linkage type between the two monosaccharides (e.g., **1** and **2**). However, the latter appears to influence the relative abundances of the $\mathbf{Y_0}$ and $\mathbf{Y_1}$ ions. The small ion at *m/z* 415 or 431 in the spectra of **2** and **3**, respectively (Figure 2a, b) corresponds to the $\mathbf{Z_1}$ ion.

Figure 3a–c show the low-energy CID product ion spectra of protonated 7-*O*-diglycosides of the flavanone type (**4**–**6**). In contrast to protonated **1**–**3**, the fragmentation patterns observed for protonated **4**–**6** are more complex. In the case of **4** (Figure 3a), for example, relatively abundant **Y** type ions are observed at *m/z* 273 (base peak, $\mathbf{Y_0}$) and 435 ($\mathbf{Y_1}$), whereas other ions at *m/z* 563 $[M + H - H_2O]^+$, 545 $[M + H - 2H_2O]^+$, 461 ($^{0,2}\mathbf{X_0}$), 417 ($\mathbf{Z_1}$), 315 ($^{0,2}\mathbf{X_0Y_1}$), 309 ($\mathbf{B_2}$), and 147 ($\mathbf{B_1}$) formed by common fragmentation routes are also present [18]. In this spectrum, the most striking feature is the presence of a Y* ion at *m/z* 419 16 units lower than the adjacent $\mathbf{Y_1}$ ion and corresponding to a neutral loss of 162 units. The high abundance of the **Y*** ion, compared with that of the regular $\mathbf{Y_1}$ ion, is unexpected on the basis of the glycan sequence. This phenomenon is even more pronounced for **5** and **6** where the **Y*** ion is the base peak at *m/z* 419 (Figure 3b) and *m/z* 449 (Figure 3c), respectively, consistent with the presence of this ion in their FAB spectra (Table 1). In addition, an ion at *m/z* 401 (**4**, **5**) or 431 (**6**) is noted which can be rationalized as the $(Y^* - H_2O)$ ion. The ion at *m/z* 315 (**4**, **5**) or 345 (**6**) can be explained by a cross-ring cleavage in the inner glucose residue and loss of the terminal rhamnose residue.

Figure 4a, b illustrate the low-energy CID product ion spectra of two protonated flavonol 3-*O*-diglycosides (**7** and **8**). The fragmentation pattern of protonated **7** and **8** is different from the spectral patterns discussed

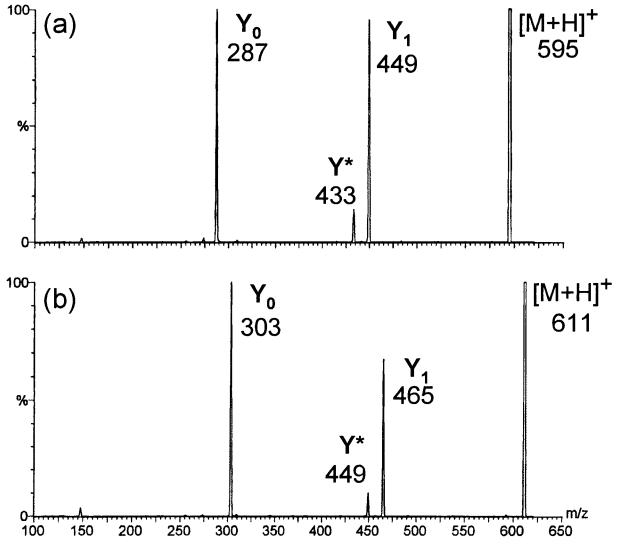

Figure 4. CID product ion spectra obtained for $[M + H]^+$ ions of (**a**) kaempferol 3-*O*-rutinoside (**7**) and (**b**) quercetin 3-*O*-rutinoside (**8**), respectively. The spectra are normalized to the most abundant product ion. The relative abundances of these ions are (**a**) 10% and (**b**) 16%, respectively.

above. Two major ions $\mathbf{Y_0}$ and $\mathbf{Y_1}$, at *m/z* 287 and 449 for **7** and at *m/z* 303 and 465 for **8**, arising from cleavage at two glycosidic bonds provide the glycan sequence as discussed for protonated **1**–**3**. However, for these two flavonol 3-*O*-rutinosides, a low abundant but readily recognizable ion (**Y***) is observed at *m/z* 433 for **7** (Figure 4a) and *m/z* 449 for **8** (Figure 4b), respectively.

It is worth mentioning that an unusual $[M + H - 162]^+$ ion (**Y***) was previously observed upon FAB [21], metastable ion fragmentation or CID [5, 22, 23] and continuous flow FAB [24] of flavonoid *O*-rutinosides or *O*-neohesperidosides, and could also be noted in desorption chemical ionization spectra [20]. From the results obtained in the present study it appears that for 7-*O*-diglycosyl flavonoids the $[M + H - 162]^+$ ion is present with a high abundance when the aglycone is a flavanone (**4**–**6**), absent when the aglycone is a flavone or flavonol (**1**–**3**), and present with a low abundance for 3-*O*-diglycosyl flavonols (**7** and **8**). This unexpected **Y*** ion corresponds to loss of the glucose residue (162 u) from the $[M + H]^+$ ion, which may cause ambiguity in the determination of the glycan sequence (e.g., for **4**–**6**) or the purity determination (e.g., for **7** and **8**) of samples, in particular, for unknown natural products isolated from plants.

Fragmentations of Protonated O-Diglycosyl Flavonoids and Mechanism of Internal Glucose Residue Loss

The **Y*** ion formed by internal glucose residue loss has, for the compounds examined in the present study containing a rutinoside or neohesperidoside part, a *m/z* value two units higher than the regular $\mathbf{Z_1}$ ion which is rationalized by loss of H_2O from the $\mathbf{Y_1}$ ion [18]. Due to its low relative abundance in most flavonoid *O*-diglycosides, this unusual **Y*** ion was often not mentioned [20, 22]. Taking into account that its mass is 16 units lower than the $\mathbf{Y_1}$ ion, the **Y*** ion can, for the compounds examined in this study, be rationalized by a rearrangement similar to that operating for the $\mathbf{Y_1}$ ion but at the other side of the glycosidic bond [21, 23, 24], i.e., it corresponds to a $(\mathbf{Y_1} - O)$ ion. On the other hand, realizing that a 162 unit mass difference between this ion and the precursor $[M + H]^+$ ion corresponds to the loss of a terminal glucose [19], the **Y*** ion may be a regular $\mathbf{Y_1}$ ion produced from a co-existing sequence isomer [5]. The first mechanistic proposal could be ruled out because it was not supported by deuterium labeling data obtained in previous experiments [5]. The second mechanistic proposal made on the basis of deuterium labeling evidence in the case of **1**, **4**, **6**, **7**, and **8**, is reasonable on a theoretical basis as it is supported by the fact that sequence isomers such as rutin (**8**) and quercetin-3-*O*-glucosyl-(1 → 2)-rhamnoside do co-occur in nature, for example, in *Saururs chinesis* [25]. However, from a phytochemical point of view the wide occurrence of a pair of sequence isomers is not expected. Particularly, co-existence of a pair of sequence isomers in samples **4**–**8** was not supported by the chromatographic data (see Experimental). Furthermore, the following findings could not be explained: (1) as the collision energy was increased, glycan fragment ions were observed, such as, at *m/z* 147 ($\mathbf{B_1}$) and 129 ($\mathbf{B_1} - H_2O$), which are consistent with a terminal rhamnose, but not with a terminal glucose, and (2) the relative abundance of the **Y*** ion was found to be dependent upon the applied collision energy, the nature of the aglycone, the linkage position at the aglycone, and the interglycosidic linkage type between the two monosaccharides. Taking into account these observations, we started to consider internal monosaccharide residue loss, a phenomenon which has been recently reported in the literature [12–16].

*(1) 7-O-Diglycosides of Flavones, Flavonols and Flavanones (**1**–**6**)*

The very simple fragmentation pattern of protonated **1** (Figure 2a) is rationalized in Scheme **1**. Protonation is believed to occur preferentially in the aglycone part, in particular, at the carbonyl oxygen atom. Charge delocalization in the C ring can lead to a protonated molecular species, which is highly stabilized by resonance. Subsequent charge-remote simple rearrangements take place resulting in the $\mathbf{Y_0}$ and $\mathbf{Y_1}$ ions at *m/z* 271 and 433, respectively, most likely involving hydrogen rearrangement from hydroxyl groups which can sterically approach the glycosidic bonds. The mechanism of $\mathbf{Y_0}$ and $\mathbf{Y_1}$ ion formation has been discussed in detail in a previous study [5]. In this study evidence for the involvement of *O*-linked hydrogen atoms has been

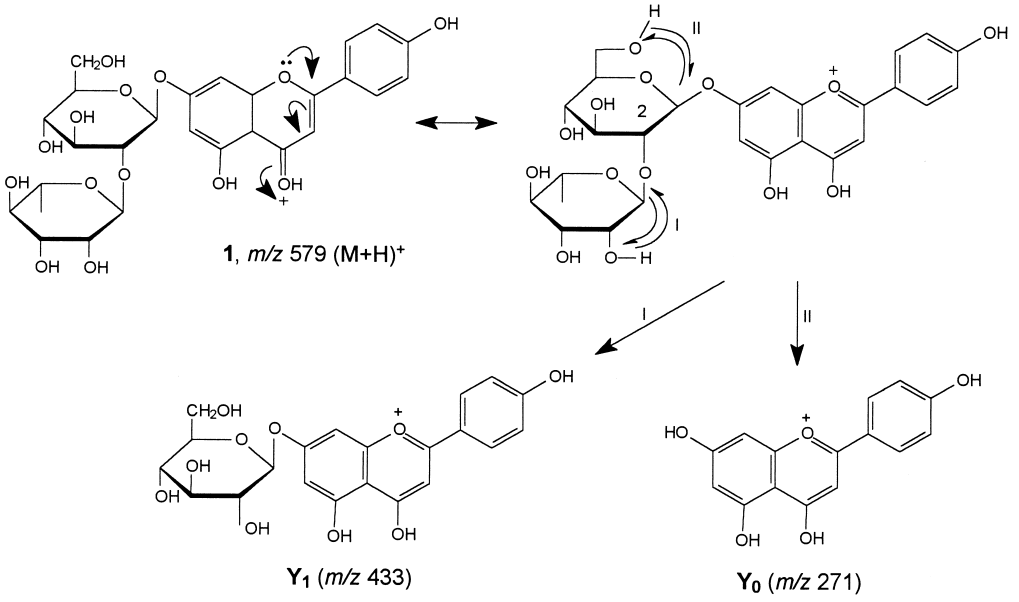

Scheme 1. Plausible mechanism for the $\mathbf{Y_0}$ and $\mathbf{Y_1}$ ions formed during CID of protonated apigenin 7-*O*-neohesperidoside (**1**).

obtained by deuterium labeling which does not support a previous mechanistic proposal that a *C*-linked hydrogen at the carbohydrate C-2 positions is eliminated [18]. Protonated **3** affords a CID spectrum (Figure 2c) very similar to that of protonated **1**, except that both the $\mathbf{Y_0}$ and $\mathbf{Y_1}$ ions show a shift of 16 mass units due to the presence of an additional hydroxyl group in the aglycone part. Because the isomers **1** and **2** only differ by the interglycosidic linkage between the two monosaccharides, the $\mathbf{Y_0}$ and $\mathbf{Y_1}$ ions for the latter can be rationalized in a similar way.

In contrast, the protonated 7-*O*-diglycosyl flavanones **4**–**6** show a relatively abundant **Y*** ion and more complex fragmentation patterns (Figure 3a–c). Comparing the CID spectra of protonated **1** and **4** (Figures 2a and 3a, respectively) which only differ by the aglycone, the relatively abundant **Y*** ion in the case of **4** can be explained on the basis of very different proton affinities of the aglycones, more specifically, of the relatively low proton affinity at the C-4 carbonyl group of aglycones of the flavanone type. It is reasonable to propose that during ionization and collisional activation the bound proton at position C-4 is mobilized and is more mobile than for protonated flavones. A plausible mechanism for the formation of the **Y*** ion in the case of protonated **4** is presented in Scheme **2**. Following migration of the proton to the terminal rhamnose part charge-induced reactions may occur leading to loss of the internal glucose residue and giving rise to the unusual **Y*** ion. The CID spectrum of the per-*O*-deuterated precursor ion species obtained in a previous study [5] showed a mass increase of 6 units for the **Y*** ion which further supports the mechanism outlined in Scheme **2**.

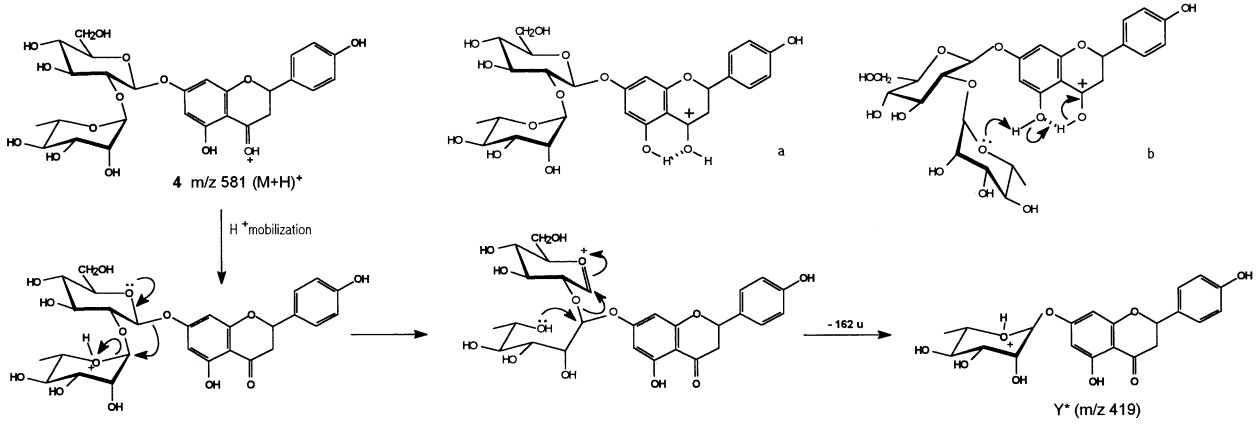

Scheme 2. Plausible mechanism for the **Y*** ion formed during CID of protonated naringenin 7-*O*-neohesperidoside (**4**).

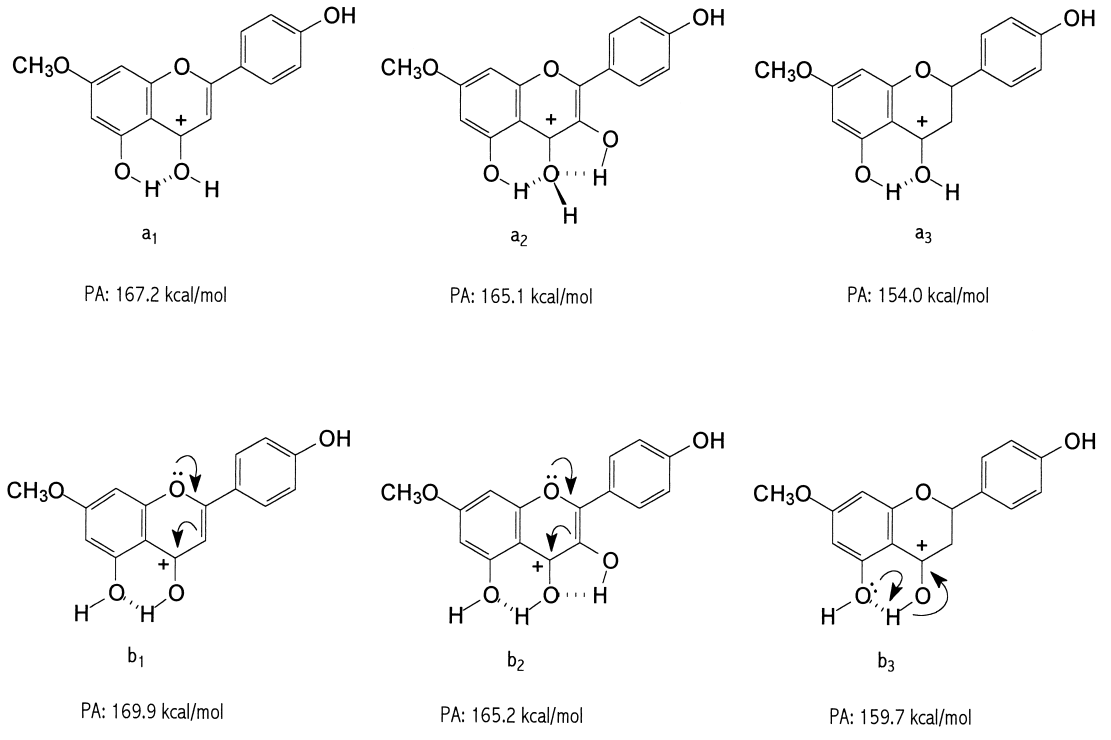

Figure 5. Representative conformers and the corresponding proton affinities (PA) values of protonated molecules of three model compounds, i.e., 7-*O*-methyl ethers of apigenin (**9**), kaempferol (**10**), and naringenin (**11**).

The mechanism proposed for protonated **4** (1,2-linkage) can also be formulated for protonated **5** and **6** (1,6-linkage). The even more pronounced formation of the **Y*** ion in the latter cases (base peak in Figure 3b, c, respectively) is likely due to a more favorable H^+ migration from the aglycone to the terminal rhamnose residue because of the presence of an additional sp^3 carbon (CH_2) between the two monosaccharide residues in the case of a 1,6-linkage, making the terminal rhamnose more flexible which is also evident from model building.

The results obtained from theoretical calculations support the mechanism proposed in Scheme **2**. In general, the primary protonation processes of a molecule can be simply modeled by molecular electrostatic potential (MEP) maps and proton affinities (PA) for ground and protonated states, respectively. The former describes electrostatic interactions between a proton (H^+) and a molecule in the early stages of the FAB ionization process, whereas the latter permits a better understanding of the stability of a proton–molecule complex formed in the gas phase. The MEP maps of three model compounds, i.e., 7-*O*-methyl ethers of apigenin (**9**, a flavone), kaempferol (**10**, a flavonol), and naringenin (**11**, a flavanone), show that the electrostatic potential at the C-4 carbonyl group of the three compounds has the maximal magnitude of the five regions of potential minima (data not shown). This means that when a proton approaches a flavonoid the incoming proton is likely trapped by the C-4 carbonyl function, leading to covalent proton–molecule complexes $\mathbf{a_1}$ (**9**), $\mathbf{a_2}$ (**10**), and $\mathbf{a_3}$ (**11**), respectively (Figure 5). Theoretical calculations of the proton affinity (PA) at different MEP minima revealed that the conformers $\mathbf{b_1}$ and $\mathbf{b_3}$, corresponding to protonation at the 5-hydroxyl function in the case of **9** and **11**, are more stable than the corresponding $\mathbf{a_1}$ and $\mathbf{a_3}$ conformers. Proton mobilization from the aglycone to the terminal rhamnose as proposed in Scheme **2** can be rationalized through the mediation of the 5-hydroxyl function (structure **b** in Scheme **2**). The significant PA difference (~10 kcal/mol) between both structures $\mathbf{b_1}$ (169.9 kcal/mol) and $\mathbf{b_3}$ (159.7 kcal/mol) explains why a protonated flavanone aglycone is less stable than the protonated flavone (or flavonol) aglycone which are stabilized by resonance (Figure 5), and may result in an enhanced proton mobilization during low-energy CID of protonated 7-*O*-diglycosyl flavanones (**4**–**6**). In addition, the ions which can be noted clearly in the CID spectra of protonated 7-*O*-diglycosyl flavanones (**4**–**6**) may also be explained, at least in part, by proton mobilization to interglycosidic O atoms and to the inner glucose and subsequent fragmentation.

(2) 3-O-Diglycosides of Flavonols (7 and 8)

A characteristic spectral feature of protonated **7** and **8** (Figure 4a, b, respectively) is that in addition to the $\mathbf{Y_0}$

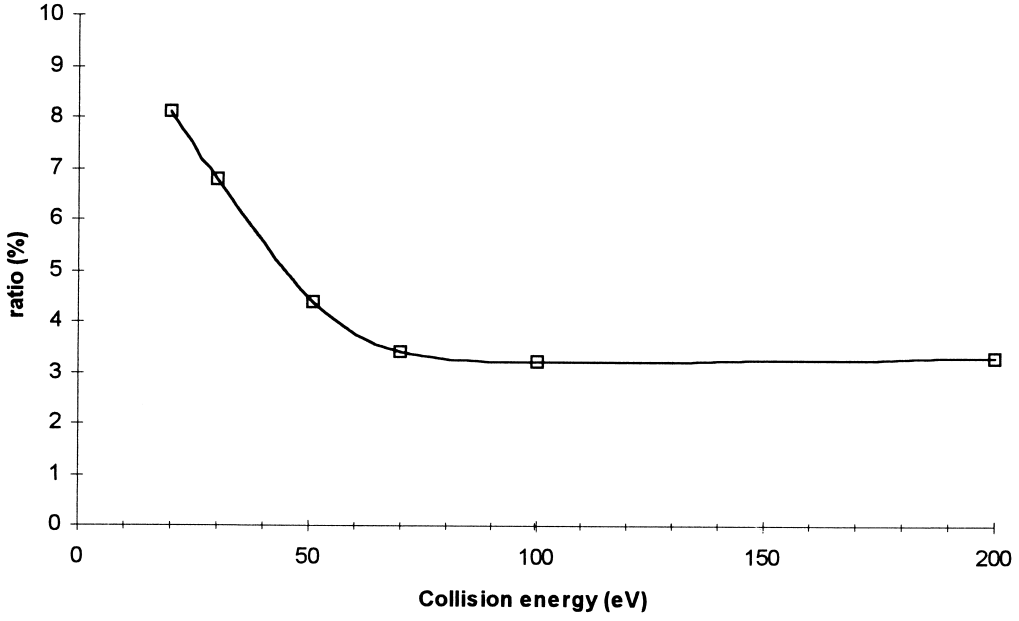

Figure 6. The ion abundance ratio of $[\mathbf{Y}^*]/\Sigma\mathbf{Y}$ vs. collision energy for protonated kaempferol 3-*O*-rutinoside (**7**).

and $\mathbf{Y}_1$ ions there is also a weak **Y*** ion. As proposed for protonated 7-*O*-diglycosides (**4**–**6**) the **Y*** ion in the case of protonated flavonol 3-*O*-diglycosides (**7** and **8**) can be rationalized by a similar mechanism involving proton mobilization from the protonated 4-carbonyl group to the terminal rhamnose residue. In order to gain insight in the energy dependence of the formation of the regular **Y**-type ions and the unusual **Y*** ion, CID experiments at different collision energies (20–200 eV) have been performed for 7-*O*-diglycosides (**1**–**3**) and 3-*O*-diglycosides (**7** and **8**). As representative examples, the CID behaviors of isomers **3** and **7** at varying collision energy are discussed here. The results show that the **Y*** ion (*m/z* 433) could not be detected for **3** in the whole collision energy (20–200 eV) range (data not shown). In the case of **7**, the relative abundance of the **Y*** ion was found to be dependent upon the collision energy. Expressing the abundance of the **Y*** ion as a percentage of the sum of abundances of all **Y** ions ($\Sigma\mathbf{Y} = [\mathbf{Y}_0] + [\mathbf{Y}_1] + [\mathbf{Y}^*]$), it can be seen that the $[\mathbf{Y}^*]/\Sigma\mathbf{Y}$ ratio decreases from 8.1% to 3.3% (Figure 6) when increasing the collision energy from 20 to 100 eV (further increasing the collision energy to 200 eV does not change the ratio, but increases the abundances of glycan related ions). The formation of the **Y*** ion is favored at a relatively low collision energy (typically $<$50 eV), which is in agreement with previous findings that the **Y*** ion is a rearrangement ion [13, 14, 16].

Conclusions

An unusual $[M + H - 162]^+$ ion was observed upon low-energy CID of protonated *O*-diglycosyl flavonoids. Previous deuterium labeling studies revealed that it is a rearrangement ion, directly formed from protonated molecules by loss of a neutral glucose residue [5]. Results obtained in the present study show that the formation of this $[M + H - 162]^+$ ion is substantially affected by the nature of the flavonoid aglycone. A plausible mechanism is proposed involving mobilization of the proton from the aglycone to the disaccharidic part of the flavonoid *O*-diglycosides. The proposed mechanism was supported by theoretical calculations and model building.

Acknowledgments

We gratefully acknowledge the financial support by the Fund for Scientific Research (Belgium-Flanders; FWO; grant no. 6.0082.98) and the Concerted Actions of the Regional Government of Flanders (grant no. 99/3/34). M.C. is indebted to the FWO as a research director.

References

1. Harborne, J. B. *The Flavonoids*; Chapman & Hall: London, 1988.
2. Harborne, J. B. *The Flavonoids: Advances in Research Since 1986*; Chapman & Hall: London, 1994.
3. Li, Q. M.; Van den Heuvel, H.; Delorenzo, O.; Corthout, J.; Pieters, L. A. C.; Vlietinck, A. J.; Claeys, M. *J. Chromatogr. B* **1991,** *562*, 435–446.
4. Li, Q. M.; Van den Heuvel, H.; Dillen, L.; Claeys, M. *Biol. Mass Spectrom.* **1992,** *21*, 213–221.
5. Li, Q. M.; Claeys, M. *Biol. Mass Spectrom.* **1994,** *23*, 406–416.
6. Ma, Y. L.; Li, Q. M.; Van den Heuvel, H.; Claeys, M. *Rapid Commun. Mass Spectrom.* **1997,** *11*, 1357–1364.
7. Benavente-García, O.; Castillo, J.; Marin, F. R.; Ortuno, A.; Del Río, J. A. *J. Agric. Food Chem.* **1997,** *45*, 4505–4515.
8. Gordon, M. H. *Nat. Prod. Rep.* **1996,** *13*, 265–273.

9. Shahidi, F.; Wanasundara, P. K. *Crit. Rev. Food Sci. Nutr.* **1992,** *32*, 67–103.
10. Wattenburg, L. W. *Cancer Res.* **1985,** *45*, 1–8.
11. Hertog, M. G. L.; Fesens, E. J. M.; Hollman, P. C. H.; Katan, M. B.; Kromhout, D. *Lancet* **1993,** *342*, 1007–1011.
12. Kováčik, V.; Hirsch, J.; Kováč, P.; Heerma, W.; Thomas-Oates, J.; Haverkamp, J. *J. Mass Spectrom.* **1995,** *30*, 949–958.
13. Brüll, L. P.; Heerma, W.; Thomas-Oates, J.; Haverkamp, J.; Kováčik, V.; Kováč, P. *J. Am. Soc. Mass Spectrom.* **1997,** *8*, 43–49.
14. Brüll, L. P.; Kováčik, V.; Thomas-Oates, J. E.; Heerma, W; Haverkamp, J. *Rapid Commun. Mass Spectrom.* **1998,** *12*, 1520–1532.
15. Ernst, B.; Müller, D. R.; Richter, W. J. *Int. J. Mass Spectrom. Ion Processes* **1997,** *160*, 283–290.
16. Warrack, B. M.; Hail, M. E.; Triolo, A.; Animati, F.; Seraglia, R.; Traldi, P. *J. Am. Soc. Mass Spectrom.* **1998,** *9*, 710–715.
17. Vande Casteele, K.; Geiger, H.; Van Sumere, C. F. *J. Chromatogr.* **1982,** *240*, 81–94.
18. Domon, B.; Costello, C. *Glycoconjugate J.* **1988,** *5*, 397–409.
19. Stewart, J. J. P. *J. Comput. Aided Mol. Des.* **1990,** *4*, 1–105.
20. Domon, B.; Hostettmann, K. *Phytochemistry* **1985,** *24*, 575–580.
21. Sakushima, A.; Nishibe, S.; Takeda, T.; Ogihara, Y. *Mass Spectrosc.* **1988,** *36*, 71–80.
22. de Koster, C. G.; Heerma, W.; Dijkstra, G.; Niemann, G. J. *Biomed. Mass Spectrom.* **1985,** *12*, 596–601.
23. Crow, F. W.; Tomer, K. B.; Looker, J. H.; Gross, M. L. *Anal. Chem.* **1986,** *155*, 286–307.
24. Sumner, L. W.; Paiva, N. L.; Dixon, R. A.; Geno, P. W. *J. Mass Spectrom.* **1996,** *31*, 472–485.
25. Sung, S. H.; Kim, Y. C. *Abstracts of the 39th Annual Meeting of the American Society of Pharmacognosy*; Orlando, FL, July 1998.